Quantitative Analysis of Cadherin-Catenin-Actin Reorganization during Development of Cell–Cell Adhesion

Cynthia L. Adams, W. James Nelson, and Stephen J Smith

Department of Molecular and Cellular Physiology, Stanford University School of Medicine, Stanford, California 94305-5426

Abstract. Epithelial cell–cell adhesion requires interactions between opposing extracellular domains of E-cadherin, and among the cytoplasmic domain of E-cadherin, catenins, and actin cytoskeleton. Little is known about how the cadherin-catenin-actin complex is assembled upon cell–cell contact, or how these complexes initiate and strengthen adhesion. We have used time-lapse differential interference contrast (DIC) imaging to observe the development of cell–cell contacts, and quantitative retrospective immunocytochemistry to measure recruitment of proteins to those contacts. We show that E-cadherin, α-catenin, and β-catenin, but not plakoglobin, coassemble into Triton X-100 insoluble (TX-insoluble) structures at cell–cell contacts with kinetics similar to those for strengthening of E-cadherin–mediated cell adhesion (Angres, B., A. Barth, and W.J. Nelson. 1996. *J. Cell Biol.* 134:549–557). TX-insoluble E-cadherin, α-catenin, and β-catenin colocalize along cell–cell contacts in spatially discrete micro-domains which we designate "puncta," and the relative amounts of each protein in each punctum increase proportionally. As the length of the contact increases, the number of puncta increases proportionally along the contact and each punctum is associated with a bundle of actin filaments. These results indicate that localized clustering of E-cadherin/catenin complexes into puncta and their association with actin is involved in initiating cell contacts. Subsequently, the spatial ordering of additional puncta along the contact may be involved in zippering membranes together, resulting in rapid strengthening of adhesion.

Cell recognition and adhesion in many cell types is mediated by cadherins which comprise a superfamily of single-transmembrane, calcium-dependent, cell adhesion proteins (Takeichi et al., 1988; Takeichi, 1991). Intercellular, homotypic cadherin binding promotes stable cell–cell adhesion (Behrens et al., 1985; Gumbiner et al., 1988; Mege et al., 1988; Nagafuchi et al., 1987) and polarized distributions of proteins in transporting epithelia (Nelson and Veshnock, 1986; Salas et al., 1988) and transfected fibroblasts (McNeill et al., 1990). Furthermore, cadherins can induce adhesion when transfected into cadherin-negative cells (Mege et al., 1988; Nagafuchi et al., 1987) and are responsible for sorting-out of mixed cell populations (Friedlander et al., 1989; Jaffe et al., 1990; Nose et al., 1988, 1990). These studies show that cadherins are at or near the top of a molecular cascade of events that generates homotypic cell–cell adhesion and initiates the structural and functional reorganization of cells.

Cadherin-mediated cell adhesion requires intracellular attachment of cadherin to the actin cytoskeleton (Hirano et al., 1987; Matsuzaki et al., 1990; Nagafuchi and Takeichi, 1988; Ozawa et al., 1989). Cadherins associate with the cytoskeleton through cytoplasmic interactions with catenins: α-catenin (102 kD), β-catenin (88 kD), and plakoglobin (80 kD) (Nagafuchi and Takeichi, 1988; Ozawa et al., 1989; Ozawa and Kemler, 1992). Plakoglobin and β-catenin share ~65% sequence homology (McCrea et al., 1991; Butz et al., 1992), yet interact with E-cadherin in mutually exclusive complexes (Hinck et al., 1994). α-Catenin has 25–30% sequence similarity to the actin-binding protein vinculin (106 kD) (Nagafuchi et al., 1991; Herrenknecht et al., 1991) and links E-cadherin to the actin cytoskeleton (Ozawa et al., 1990*a*; Rimm et al., 1995) via its association with either plakoglobin or β-catenin (Aberle et al., 1994; Jou et al., 1995). At cell–cell contacts, complexes of E-cadherin, α-catenin, and either β-catenin or plakoglobin are insoluble in Triton X-100 (TX-100),[1] suggesting an association with the cytoskeleton (Hinck et al., 1994; Nathke et al., 1994). Significantly, disruption of E-cadherin association with catenins or actin results in loss of both TX-100 insolubility and cell adhesion (Breen et al., 1994; Hirano et al., 1992; Jaffe et al., 1990; Nagafuchi and Takeichi, 1988;

Please address all correspondence to W. J. Nelson, Department of Molecular and Cellular Physiology, Stanford University School of Medicine, Stanford, CA 94305-5426. Tel.: (415) 725-7596. Fax: (415) 498-5286. E-Mail: wjnelson@leland.stanford.edu

1. *Abbreviations used in this paper*: DIC, differential interference contrast; FIR, Fluorescence Intensity Ratio; TX-100, Triton X-100; TX-insoluble, Triton X-100 insoluble.

© The Rockefeller University Press, 0021-9525/96/12/1899/13 $2.00

Oyama et al., 1994; Ozawa et al., 1989, 1990; Shimoyama et al., 1992; Stappert and Kemler, 1994; Tsukita et al., 1992).

Important advances have been made in characterizing components of the cadherin/catenin complex, identifying binding partners in the complex, and substantiating the requirements for the complex in cell adhesion. In contrast, little is known about the temporal and spatial regulation of complex formation during the initiation and strengthening of cell–cell adhesion. Initial studies by McNeill et al. (1993) showed a delay of E-cadherin recruitment into a TX-insoluble pool at newly established cell–cell contacts. More recently, Angres et al. (1996) have shown, using a quantitative adhesion assay, that strengthening of adhesion occurs over a 30–40-min period after initiation of cell–cell contacts. However, it is unclear how TX-insoluble E-cadherin assembles as a complex with catenins on the cell surface during cell–cell adhesion, whether the cadherin/catenin complex is attached to the actin cytoskeleton before, or following cell–cell contact, or how these protein interactions initiate and strengthen adhesion.

Using multi-site time-lapse different interference contrast (DIC) imaging followed by quantitative retrospective immunocytochemistry, we analyzed the accumulation of TX-insoluble E-cadherin, α-catenin, β-catenin, and plakoglobin, and the redistribution of actin at individually monitored sites of new contact between MDCK epithelial cells. We show that TX-insoluble α-catenin and β-catenin coaccumulate at initial contact sites with E-cadherin, within minutes of initial contact, whereas plakoglobin accumulation at such sites is greatly delayed. Furthermore, proportional amounts of TX-insoluble E-cadherin, α-catenin, and β-catenin exist as discrete "puncta" along cell–cell contacts. We also describe the distribution of actin bundles relative to these puncta in newly formed contacts. These results provide a detailed picture of the temporal and spatial dynamics of recruitment of cadherins, catenins, and actin sites of cell–cell contact. Based on these and earlier studies (Angres et al., 1996; McNeill et al., 1993), we propose a mechanism involving these complexes in initiating and strengthening cell–cell adhesion.

Materials and Methods

Cell Culture

MDCK GII cells (Mays et al., 1995) were maintained in tissue culture plastic at low density in DMEM and 10% FBS (Gemini, Calabasas, CA). Cells were removed with trypsin for 5 min, resuspended in DMEM, and plated on collagen-coated coverslips at a density of 2–4 × 10^5 cells/ml (for details see Nelson and Veshnock, 1986).

Multi-Site DIC Microscopy

4–6 h after plating, the culture medium was replaced with Modified Essential Medium with Earle's salts (movie buffer). The coverslip was transferred to a closed viewing chamber and bathed in 500 μl movie buffer. The chamber was placed on a robotic stage (designed and built by Drs. Noam Ziv and Stephen Smith) attached to a scanning laser confocal and DIC microscope (designed and built by Dr. Stephen Smith). Twelve sites on the coverslip were chosen, the x-y coordinates were saved, and the sites were robotically revisited in sequence during the automated time-lapse recording (see below). Nomarski images were collected with a transmitted light detector at 488 nm illumination at <25 μW using a Zeiss (Carl Zeiss, Inc., Thornwood, NY) 25× NA 0.8 objective, and stored digitally.

Time-lapse Recording

By integrating automated robotic stage control with image collection functions, a digital DIC image was automatically recorded at each site once every 2–4 min. This resulted in the collection of 15–30 images per site over 1 h. After recording, the files were collated into digital movie sequences (Microsoft Video 1, Cinepack or motion JPEG formats) using Premiere (Adobe Systems Inc., Mountain View, CA) or Microsoft Windows software written by Dr. Noam Ziv. Movies were used to identify and calculate the age of cell contact events. Within the 1-h viewing period, 5–30 cell–cell contacts were usually formed.

Retrospective Immunocytochemistry

At the end of the viewing period, cells were processed in the viewing chamber as follows: extract in CSK buffer (50 mM NaCl, 10 mM Pipes, pH 6.8, 3 mM $MgCl_2$, 0.5% Triton X-100, 30 mM sucrose) for 5 min at 4°C; wash for 5 min in PBS; fix in 4% wt/vol formaldehyde in PBS; wash for 5 min in PBS; block for 25 min in 50 mM NH_4Cl, 0.5% BSA, 0.1% goat serum, 1 mM glycine buffered with PBS. All subsequent incubations were performed in PBS containing 0.5% BSA, and 0.1% goat and donkey sera (blocking buffer). Cells were incubated overnight at 4°C with combinations of rabbit and mouse antibody: rabbit polyclonal anti-peptide antibodies raised to either α-catenin, β-catenin, or plakoglobin and affinity-purified using cognate peptide (Hinck et al., 1994); monoclonal antibodies to either β-catenin (Transduction Laboratories, Lexington, KY) or E-cadherin (antibody 3G8 kindly provided by Dr. Warren Gallin, University of Alberta, Alberta, Canada). After a 30-min wash in blocking buffer, cells were labeled for 1 h at room temperature with FITC anti–rabbit (Jackson ImmunoResearch Laboratories, West Grove, PA) or FITC-conjugated phalloidin (Molecular Probes, Eugene, OR), and CY5 anti–mouse (Biological Detection Systems, Inc., Pittsburgh, PA); all antibodies were diluted in blocking buffer. After a 30-min wash with blocking buffer, the chamber was filled with PBS or Vectasheild (Vector Laboratories, Burlingame, CA), and then returned to the microscope. Fig. 1 illustrates different stages of processing live cells for immunofluorescence microscopy; note that the morphology of cell–cell contacts is well preserved following extraction with Triton X-100 and fixation.

Fluorescence Imaging

Fluorescence and DIC images from the original 12 sites were recorded using a Zeiss Plan-Neofluar 25× NA 0.8 objective. For each contact, high magnification, three-dimensional images were collected as sets of 10 confocal optical sections at 0.5 micron intervals using a Nikon PlanApo 60× NA 1.40 objective. CY5 images were excited at 632 nm with a helium neon laser, and emissions were collected through a 650-nm long-pass filter. FITC label was excited at 488 nm with an argon ion laser, and collected through a 510–550-nm band-pass filter.

Image Analysis

Age of Contact and Punctum. The timing of initial contacts between cells under DIC time-lapse observation was determined by identifying the first frame in which the two cells appeared to share a continuous membrane. Ages of contacts for retrospective analyses were calculated as the time elapsing between initial contact and the time of fixation (see also, McNeill et al., 1993). Ages of individual puncta were determined similarly from detailed analyses of the spatial expansions of contacts as observed by time-lapse DIC microscopy. Puncta containing cadherin and catenins were identified by retrospective immunocytochemistry (see above) and mapped to a section of the contact in the corresponding DIC image (see Results, Fig. 8 *A*).

Fluorescence Intensity Ratio. For most quantitative fluorescence measurements, three-dimensional images of the contact site were reduced to two-dimensional projections by adding all optical section images using MetaMorph software (Universal Imaging Corp., West Chester, PA). To calculate the average accumulation of protein in a contact, regions of equal area were drawn around the brightest areas of the contact (contact site; Fig. 4 *a*, region 1), the edge of a membrane not involved in cell–cell contact (noncontacting membrane; Fig. 4 *a*, region 2), and a cell-free area of the coverslip (background; Fig. 4 *a*, region 3). Fluorescence intensity ratio (FIR) was calculated using Microsoft Excel (Microsoft, Redmond, WA): FIR = (contact site − background) / (membrane − background). If a protein had not accumulated in the contact region relative to noncontacting membrane, FIR at a contact site should be 2 (i.e., combined stain-

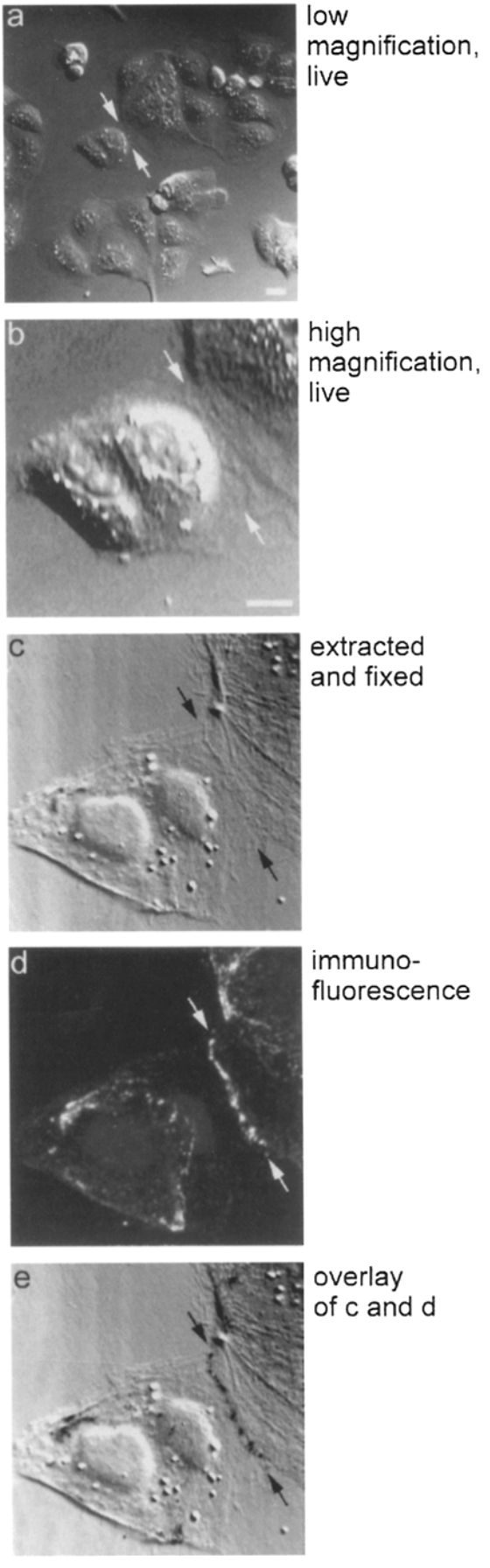

ing of two closely opposed membranes); similarly, a FIR >2 reflects an accumulation of protein in the contact area compared to noncontacting membrane.

FIR value of a given punctum was calculated by using the intensity value in a 500-nm region drawn around the region of localized bright intensity within the contact area. This region was best identified by viewing the fluorescence image in pseudocolor rendering. Background and membrane intensities were taken by averaging 15 areas of the same size in cell and contact free areas, respectively. FIR was calculated as described above.

Results

Time Course of Recruitment of TX-insoluble E-Cadherin, α-Catenin, β-Catenin, and Plakoglobin to Cell–Cell Contacts

Before embarking on an analysis of recruitment of E-cadherin and catenins into contact sites, we examined staining patterns of total and TX-insoluble proteins in cells that had been cultured for 24 h. Fig. 2 compares E-cadherin, α-catenin, β-catenin, and plakoglobin immunofluorescence in cells that were either fixed in formaldehyde before extraction in TX-100 (*total protein*; Fig. 2, *a*, *c*, *e*, and *g*), or extracted in TX-100 and then fixed in formaldehyde (*TX-insoluble protein*; Fig. 2, *b*, *d*, *f*, and *h*); cells were labeled with E-cadherin (*a* and *b*), β-catenin (*c* and *d*), α-catenin (*e* and *f*), or plakoglobin (*g* and *h*) antibodies. After extraction with TX-100, significant amounts of E-cadherin, α-catenin, β-catenin, and plakoglobin were removed from the cytoplasm and noncontacting plasma membrane (compare staining indicated by arrows in *c* and *d*), whereas significant amounts of these proteins persisted at established cell–cell contact sites (compare staining indicated by arrows in *e* and *f*). These data show that, like E-cadherin, TX-100 soluble catenins are distributed throughout the cell, while TX-100 insoluble catenins are preferentially found at cell–cell contacts.

We examined the time course of recruitment of TX-insoluble E-cadherin, α-catenin, β-catenin, and plakoglobin to contact sites during initial stages of cell–cell adhesion (<1 h old). Multi-site time-lapse recording was used to capture the formation of multiple contacts during a viewing period; since contacts form at different times during this period, the record includes contacts of different ages. Each contact that had formed during the time-lapse recording was double-labeled with a combination of two antibodies against either E-cadherin, α-catenin, β-catenin, or plakoglobin, and a fluorescence intensity ratio (FIR) was calculated for each antibody (for details see Materials and Methods).

Figs. 3 and 4 show a detailed analysis of immunofluores-

Figure 1. Experimental Design. (*a*) Example of the last frame of one of 12 fields of live cells used in a multi-site time-lapse imaging experiment. Arrows point to a 33-min-old contact formed during the recording. Arrows in all panels point to same contact area. (*b*) Zoomed image of the contact marked in *a*. (*c*) DIC image of the same contact after extraction in 0.5% TX-100 and fixation in formaldehyde. (*d*) Retrospective staining with E-cadherin primary antibody (3G8) and CY5-anti–mouse secondary antibody. (*e*) Overlay of DIC image (*c*) and retrospective immunofluorescence image of E-cadherin staining (*d*). Bar, 10 μm.

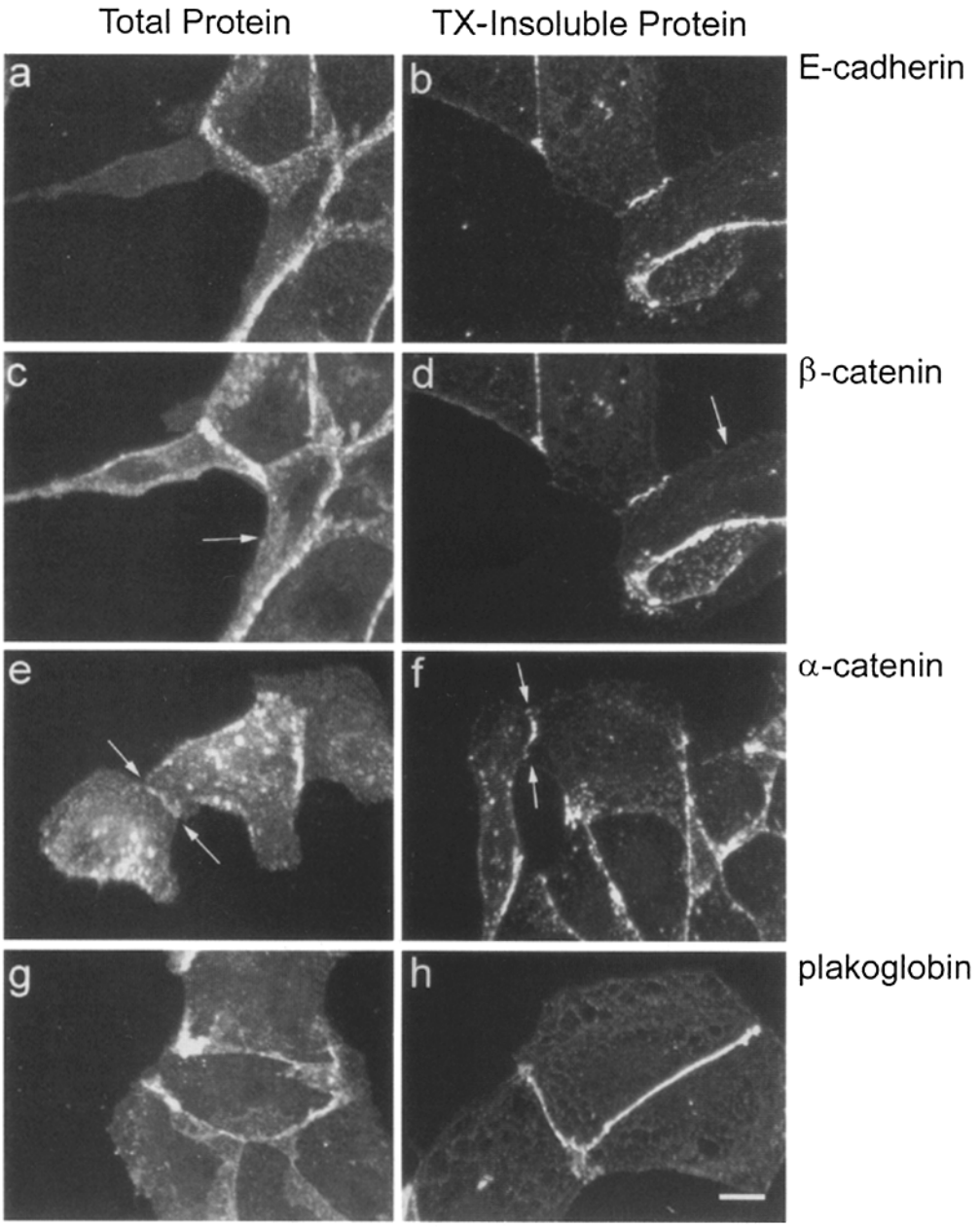

Figure 2. Comparison of total and TX-insoluble E-cadherin, β-catenin, α-catenin, and plakoglobin immunofluorescence in MDCK cells. Cells were plated on collagen-coated coverslips and processed 24 h later for immunofluorescence microscopy. *a*, *c*, *e*, and *g* show cells fixed in 4% formaldehyde and then permeabilized with 0.5% TX-100. *b*, *d*, *f*, and *h* show cells extracted in 0.5% TX-100 and then fixed in 4% formaldehyde. Immunofluorescence staining of E-cadherin (*a* and *b*), β-catenin (*c* and *d*), α-catenin (*e* and *f*), and plakoglobin (*g* and *h*) of total protein and TX-insoluble soluble protein are shown, respectively. Arrows in *c* and *d* point to noncontacting membrane; arrows in *e* and *f* point to the edges of mature contacts. Bar, 10 μm.

cence staining and FIR for contacts between 1 and 40 min old. Fig. 3 shows representative immunofluorescence images of cell–cell contacts labeled with E-cadherin (*a* and *b*), β-catenin (*c* and *d*), α-catenin (*e* and *f*), or plakoglobin (*g* and *h*); the contacts identified between arrows are 5 min (*a*, *c*, *e*, and *g*) or 20 min (*b*, *d*, *f*, and *h*) old. Note that TX-insoluble protein in 5-min-old contacts is undetectable, while significant amounts of TX-insoluble E-cadherin, α-catenin, and β-catenin, but not plakoglobin, are detectable in 20-min-old contacts. To quantitate these relationships, we calculated FIR for each protein at many different contact ages.

Fig. 4 *a* shows representative areas used to calculate FIR. Fig. 4 *b* shows averaged FIR as a function of contact age for E-cadherin (*circles*), α-catenin (*squares*), β-catenin (*triangles*), and plakoglobin (*diamonds*) from 300 contacts. Fig. 4 *c* gives the number of FIR calculations for each protein performed for different contact ages from different contacts, and the averaged FIR values ± SEM. Results show that amounts of TX-insoluble E-cadherin, α-catenin, and β-catenin increased 2–4-fold at contact sites within 45 min of cell–cell contact. In contrast, plakoglobin FIR did not increase significantly in contacts during this time; note that plakoglobin accumulates at older contact sites (compare contact marked in Fig. 3 *h* with other, older contacts in the same field). We conclude that E-cadherin, α-catenin, and β-catenin rapidly enter a TX-insoluble pool of proteins at contact sites and that this is temporally coordinated. In contrast, TX-insoluble plakoglobin accumulates at later times of contact development (see Discussion).

E-Cadherin and Catenin Staining at Newly Formed Cell–Cell Contacts Is Punctate

Our observations of newly formed cell–cell contact sites strongly suggest that specific molecular adhesion is medi-

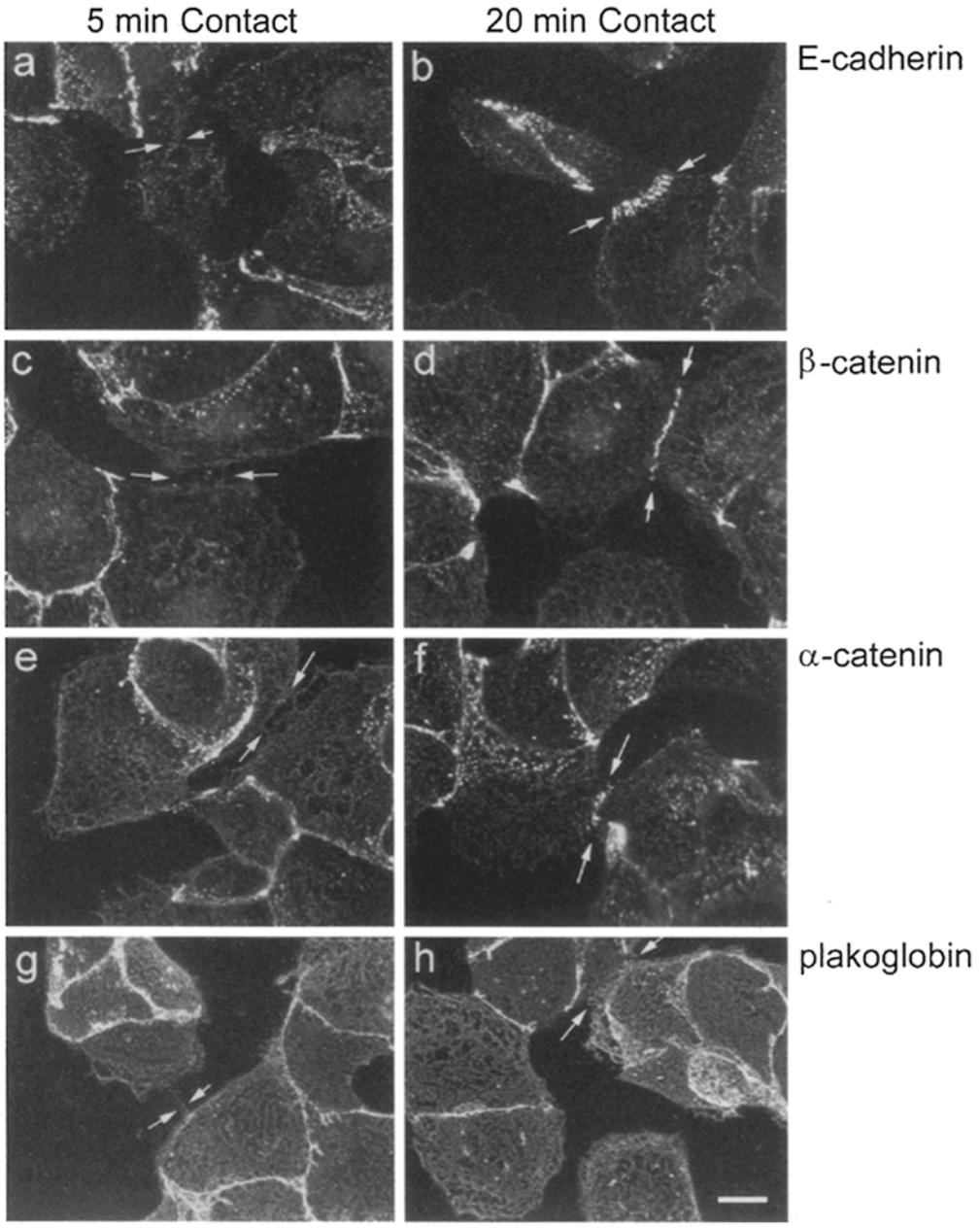

Figure 3. Retrospective immunofluorescence staining of E-cadherin, β-catenin, α-catenin, and plakoglobin in contacts 5 and 20 min old. Multisite time-lapse DIC images were recorded for 60 min, and the ages of contacts formed were determined. Cells were then extracted in 0.5% TX-100, fixed in 4% formaldehyde, and stained with either E-cadherin, β-catenin, α-catenin, or plakoglobin antibody. *a*, *c*, *e*, and *g* show examples of retrospective staining of 5-min-old contacts; *b*, *d*, *f*, and *h* show 20-min-old contacts. E-Cadherin (*a* and *b*), β-catenin (*c* and *d*), α-catenin (*e* and *f*), and plakoglobin (*g* and *h*) staining of TX-insoluble protein at 5 and 20 min are shown, respectively. Arrows in all panels point to the edges of the newly formed (5 or 20 min) contact area. Bar, 10 μm.

ated by a discrete punctate structure. Immunofluorescence images representing distributions of TX-insoluble E-cadherin, α-catenin, and β-catenin at young contacts invariably exhibited discrete fluorescence "hotspots" which always coincided exactly for each of the three proteins. Figs. 4 and 5 illustrate representative observations. TX-insoluble E-cadherin immunofluorescence appeared distinctly punctate, rather than continuous, in the 45-min-old contact shown in Fig. 4 *a*. E-cadherin and α-catenin staining precisely colocalize into similar punctate structures marked by the arrows in Fig. 5, row *4*. β-Catenin also colocalizes with E-cadherin and α-catenin into discrete puncta, while plakoglobin staining appears more reticular (data not shown). While we were initially concerned that the puncta evident in these immunofluorescence analyses might be artifacts of the extraction or chemical fixation procedures used, observations of precisely corresponding punctate features in DIC images of live cells have convinced us that these puncta must have substantial, nonartifactual reality.

Fig. 5 shows examples of the appearance of punctate structures during contact formation. Our observations of contact formation using time-lapse DIC images are similar to those described by McNeill et al. (1993): transient testing of two noncontacting membranes, stabilization of a contact between two small (1–2 μm) areas, then gradual "zippering" together of those opposing membranes. The stabilization or nucleation of contact formation is usually demarcated by a punctate structure in the membrane that can be identified by DIC microscopy (*arrows*, Fig. 5, row *2*). As the membranes zipper together in both directions, additional punctate regions form along the increasing surface area of the contact (*arrows*; Fig. 5, row *3*).

Retrospective E-cadherin and α-catenin staining of the contacts formed in Fig. 5 reveals immunofluorescent

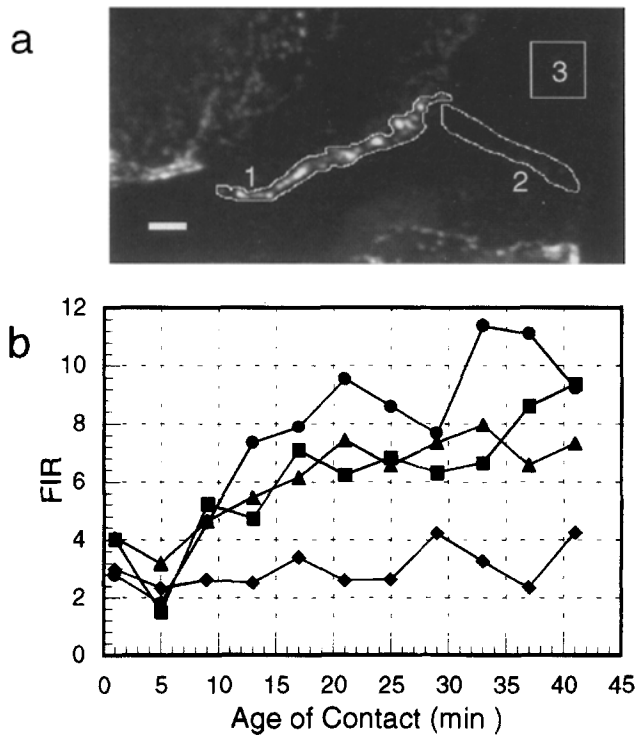

c

Age of contact (min.)	E-cadherin n	E-cadherin FIR +/- SEM	Alpha-catenin n	Alpha-catenin FIR +/- SEM	Beta-catenin n	Beta-catenin FIR +/- SEM	Plakoglobin n	Plakoglobin FIR +/- SEM
1	10	2.8 +/- 0.6	6	4.0 +/- 1.5	3	4.0 +/- 1.8	4	3.0 +/- 0.3
5	9	1.8 +/- 0.4	4	1.5 +/- 0.7	3	3.2 +/- 0.7	2	2.3 +/- 0.1
9	10	4.6 +/- 1.4	6	5.2 +/- 1.6	4	4.6 +/- 0.4	5	2.6 +/- 0.7
13	4	7.3 +/- 1.9	3	4.7 +/- 0.4	9	5.4 +/- 0.7	4	2.5 +/- 0.5
17	11	7.9 +/- 2.2	4	7.1 +/- 2.4	8	6.1 +/- 0.7	7	3.4 +/- 0.6
21	15	9.5 +/- 1.9	6	6.2 +/- 1.0	4	7.4 +/- 2.6	3	2.6 +/- 0.3
25	11	8.6 +/- 1.8	6	6.8 +/- 1.8	4	6.6 +/- 1.8	7	2.6 +/- 0.3
29	14	7.6 +/- 1.8	7	6.3 +/- 1.6	4	7.3 +/- 1.4	9	4.2 +/- 0.6
33	14	11.4 +/- 2.1	14	6.6 +/- 0.8	5	8.0 +/- 1.2	5	3.2 +/- 0.2
37	12	11.1 +/- 1.7	9	8.6 +/- 0.4	5	6.6 +/- 1.4	5	2.3 +/- 0.3
41	10	9.2 +/- 2.0	7	9.4 +/- 3.0	3	7.3 +/- 3.2	5	4.2 +/- 0.5

Figure 4. Accumulation of TX-insoluble E-cadherin, β-catenin, α-catenin, and plakoglobin at newly established cell–cell contacts. (*a*) An example of the regions used to calculate fluorescence intensity ratio (FIR) of contacts: (*1*) contact site; (*2*) noncontacting membrane; (*3*) background (noncell) staining. (*b*) The age of each contact and FIR of each protein was calculated for all contacts (for details, see Materials and Methods). Graphs show the average FIR at each time point for E-cadherin (*circles*), α-catenin (*squares*), β-catenin (*triangles*), and plakoglobin (*diamonds*). The table in *c* summarizes the number (*n*) of contacts used to calculate the average FIR ± SEM for each age of contact. Bar: (*a*) 10 μm.

puncta which have a similar distribution pattern as the punctate features in row *3* (*arrows*; Fig. 5, row *4*). The overlay of images in row *4* on row *3* (Fig. 5, row *5*) shows that many discrete regions of TX-insoluble E-cadherin and α-catenin precisely colocalize with the punctate features highlighted in row *3*. The punctate structures seen in the DIC images may be due to thickening of membrane in that region, or localized increase in the concentration of protein resulting in an increase in the index of refraction. Immunofluorescent puncta which do not correspond to punctate features in the last DIC image (*open arrows*; Fig. 5, columns *B* and *D*) may be very young, or the underlying structure may be small and obscured by raised membrane surrounding the punctum.

The apparent sizes of the observed immunofluorescent puncta are quite uniform. Importantly, however, this size is too small to be at or near the resolution limit for standard confocal microscopy techniques. The uniformity of puncta size therefore may simply reflect the inability to resolve directly the true size of subresolution structures. While the present observations seem to justify a conclusion that molecular adhesion at early stages of cell–cell contact reflect discrete and separate punctate structures, additional work, probably at the electron microscopic level, will be necessary to determine the true sizes of these puncta.

The observation that TX-insoluble E-cadherin, α-catenin, and β-catenin colocalize exclusively in puncta along cell–cell contacts suggests that these puncta are involved in cell–cell adhesion. To examine the spacing of these puncta, we calculated their number as a function of contact lengths (Fig. 6 *a*). There is a linear relationship between the number of puncta and contact length. The average density of puncta is ~1 punctum/μm in contacts between 1 μm to 36 μm in length. Within a contact, the inter-particle spacing between puncta ranges from unresolvable to 4 μm. Although the density of puncta within different contact lengths is approximately constant, the spacing between punctum is not. These results suggest that as a contact zippers together and the length of the contact increases, new puncta are added along the contact at a constant the average density over the course of an hour.

The number of puncta appears to be strongly correlated with the age of contact. However, a scatter plot of age vs contact length shows that length varies considerably at any given age (Fig. 6 *b*). For example, at 5 min the range of contact lengths is 1–10 μm, while at 49 min contact lengths range from 5 to 25 μm. These data show that contact lengths increase at different rates (5–30 μm/h). Therefore, the number of puncta in a contact is related to the rate that the contact zippers together, rather than to the age of the contact. While there is an accumulation of the number of puncta over time, the number of puncta is linearly related to the length of the contact, and increase in number as the length of the contact increases over time.

Relative Amounts of TX-insoluble E-Cadherin, α-Catenin and β-Catenin Accumulate Proportionally in Puncta

Since E-cadherin, α-catenin, and β-catenin colocalize in discrete puncta, we asked whether the amounts of each protein are proportional within each punctum. To quantitate this relationship, FIR values were measured for each antibody in each punctum along a contact that was double-labeled with different combinations of antibodies (see Materials and Methods). Fig. 7 shows representative relationships between FIR values of E-cadherin and α-catenin (Fig. 7 *a*), α-catenin, and β-catenin (Fig. 7 *b*), and β-catenin and plakoglobin (Fig. 7 *c*) in every punctum along three contacts. Results show that amounts of E-cadherin, α-catenin, and β-catenin are proportional. However, plakoglobin does not accumulate in significant amounts in contacts less than 30-min old compared to β-catenin (Fig. 7

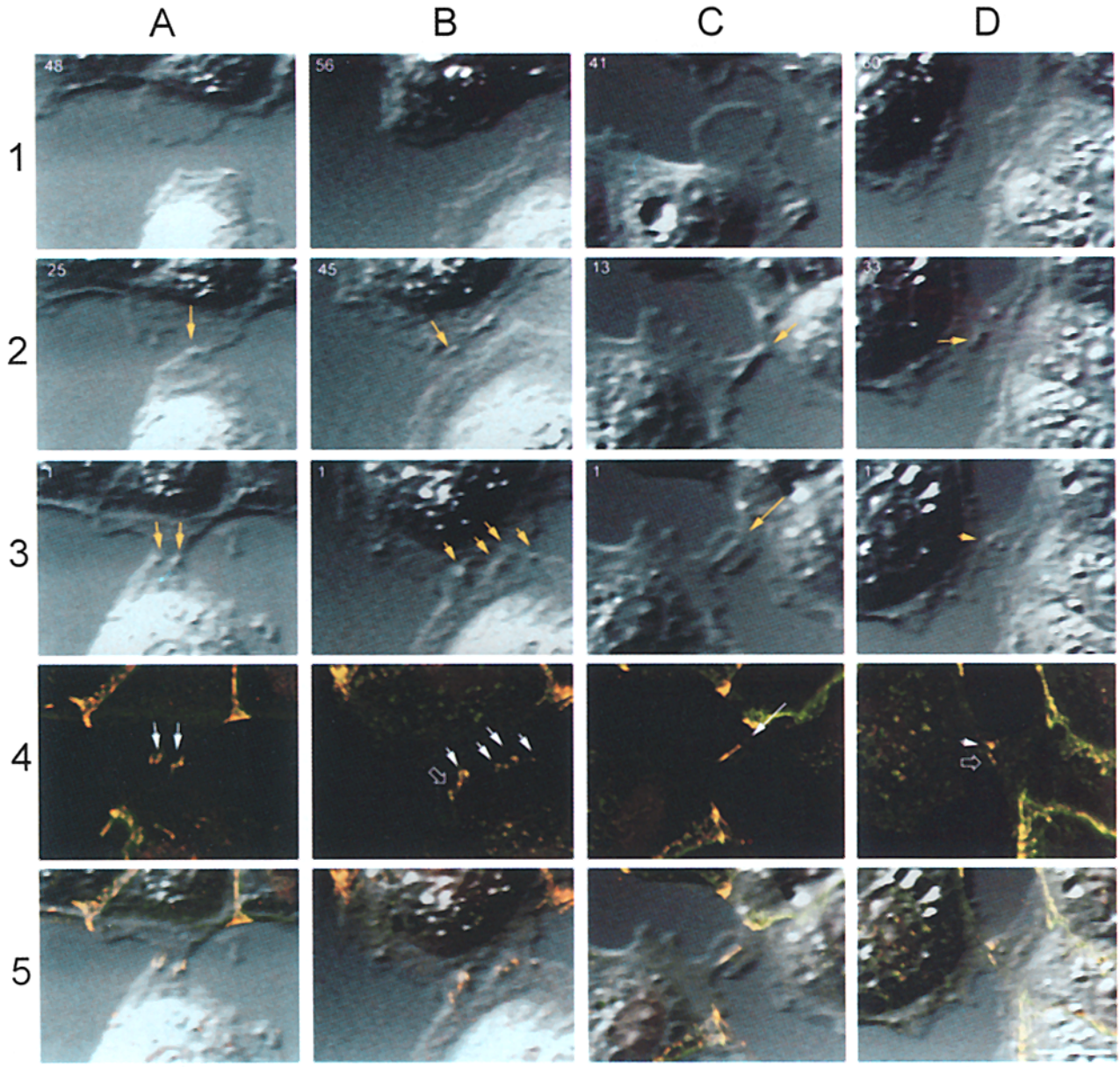

Figure 5. DIC and immunofluorescent puncta during contact formation. Columns *A–D* show four examples of contact formation between two cells. Rows *1–3* show three frames from different times during the video imaging; the amount of time remaining (min) before fixation is shown in the upper left hand corner. The arrows in row *2* point to the nucleation point of the contact (see Results). Arrows in row *3* point to DIC puncta along the length of the contact just before fixation. Cells were processed as described (see Materials and Methods) and stained for E-cadherin and α-catenin. Row *4* shows retrospective immunofluorescence of cells in row *3*; E-cadherin (*red*, CY5) and α-catenin (*green*, FITC). Note that the CY5-anti–mouse antibody in the absence of primary antibody showed staining of nuclei; other antibodies did not label the nucleus, even in the presence of primary antibodies. Arrows in row *4* are at the same positions as in row *3* and point to immunofluorescent puncta in the contact. Row *5* shows the overlay of the immunofluorescence in row *4* on the last live DIC image in row *3*. Note the overlap of DIC and immunofluorescent puncta in row *5*. Occasionally, we also observed two other general types of contact in which either one or both contacting cell edges remained rounded up (data not shown). Since it was difficult to observe punctate regions in these types of contacts because of the rounded cell surface, they were excluded from this analysis. Bar: (row *5*) 10 μm.

c). While we do not know the absolute stoichiometry of proteins in puncta, these data indicate that the stoichiometry is constant within a population of puncta.

The increase of average FIR of contacts may be due to an increase in either the total number of puncta along the contact, or amount of protein in individual puncta. Time-lapse recordings of cell–cell contacts allow us to differentiate between these possibilities. As a contact matures (Fig. 8 *A*, *a–d*), two opposing cell membranes zipper together such that, at the time of fixation, different parts of membrane have been in contact for different times. The age along the length of the developing contact is shown schematically (Fig. 8 *A*, *e*). To calculate the age of each punctum within a contact, we referred to consecutive frames of

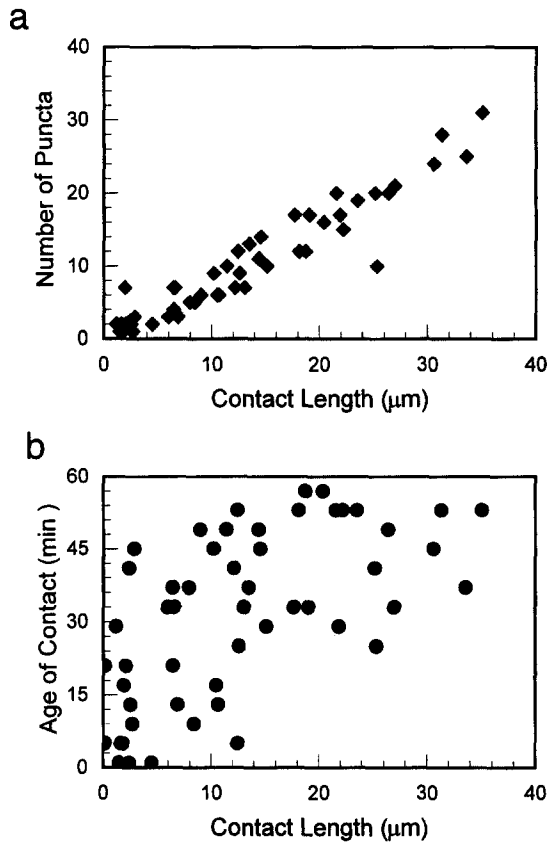

Figure 6. Distribution of TX-100 insoluble E-cadherin puncta along sites of cell–cell contact. The number of puncta, and the length, age, and FIR of newly formed contacts were calculated (Materials and Methods). Graph *a* shows the scatter plot of the number of puncta vs contact length for 50 different contacts. Graph *b* shows the scatter plot of contact age vs contact length.

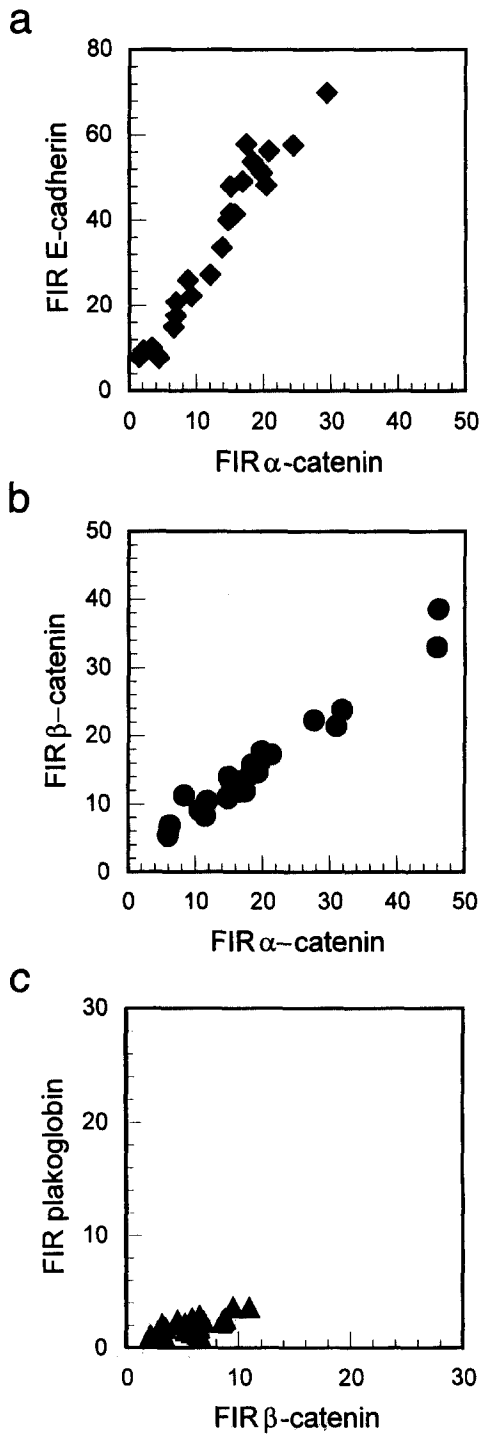

Figure 7. Relative amounts of E-cadherin, α-catenin, β-catenin, and plakoglobin in puncta. FIR values of proteins in each punctum in a contact were calculated for both antibodies used in a double-labeling experiment (see Materials and Methods). Graphs *a–c* are scatter plots of the FIR values of individual puncta in one contact. Graphs show the scatter plot of FIR values of each punctum in a contact for E-cadherin and α-catenin (*a*), β-catenin and α-catenin (*b*), and plakoglobin and β-catenin (*c*).

the DIC movie (Fig. 8 *A*, *a–d*), assigned an age to each segment of a contact as it appeared (Fig. 8 *A*, *e*), and, thereby, determined the age of all immunofluorescent puncta within the contact area (Fig. 8 *A*, *f*). The oldest part of the contact (<40 min) is delineated between red lines running down Fig. 8 *A*; several puncta are detected within this region (Fig. 8 *A*, *f*). The region of the contact that is 10–25-min old is delineated between the green and yellow lines, and several puncta are present. No puncta are detected in the region of the contact less than 10-min old, which is delineated between the green and blue lines, although the cells are clearly in contact in this area (Fig. 8 *A*, *d*). When the immunofluorescent puncta from Fig. 8 *A*, *f* are color-coded for intensity, the brightest puncta (pseudocolor yellow, Fig. 8 *A*, *g*) are generally in the oldest regions of the contact, while the dimmer puncta are in the new regions of the contact (pseudocolor blue, Fig. 8 *A*, *g*). Notice also that the immunofluorescent puncta overlap with distinctly raised features in the DIC images (compare Fig. 8 *A*, *d* and *f*); these features are in the oldest part of the contact and absent in the newest parts (Fig. 8 *A*, *d*).

Since the fluorescence intensity of puncta can be assigned to regions of the contact of known age, we examined whether there was a correlation in the FIR and age of individual puncta. Fig. 8 *B*, *a* shows immunofluorescence staining of E-cadherin in a contact that was initiated 45 min before fixation. Puncta were identified and their positions along the contact are shown in an ordinate (x, y) representation (Fig. 8 *B*, *b*). FIR of each punctum shown in

Fig. 8 *B*, *a* was measured and plotted as a function of each punctum's position (Fig. 8 *B*, *c*). In Fig. 8 *B*, *d*, the ages of each segment of the contact are plotted as a function of each punctum's position. The line running through Fig. 8 *B*, *a–d* indicates the oldest point of the contact (i.e., the site of initial nucleation of the contact). In general, the intensity of E-cadherin staining appears to increase with increasing ages of puncta; old puncta have high E-cadherin FIR, while young puncta have low FIR. To determine whether this trend holds for many contacts, FIR of TX-insoluble E-cadherin in each punctum in five different contacts was calculated and plotted as a function of punctum age (Fig. 8 *B*, *e*). Results show a gradual increase in FIR for E-cadherin in puncta that are between 1 and 20 min old; for older contacts, FIR remains approximately constant. Note that the kinetics of increase in E-cadherin FIR (Fig. 8 *B*, *e*) is similar to the kinetics of accumulation of total TX-insoluble E-cadherin at cell–cell contacts shown in Fig. 4 *b*. Thus, the kinetics of protein accumulation into the contact site does not depend on the number of puncta within a contact, but on the amount of time each punctum has been in the contact.

Puncta Are Associated with Actin at Early Cell–Cell Contacts

Formation and distribution of TX-insoluble puncta may be due to clustering of E-cadherin or catenin molecules, attachment of E-cadherin/catenin complexes to the actin cytoskeleton, or recruitment of E-cadherin and catenin molecules onto actin bundles which are in the vicinity of a developing contact. Since α-catenin binds actin and TX-100 insolubility infers association of E-cadherin with the actin cytoskeleton (for references, see Introduction), we examined the distribution of actin during formation of cell–cell contacts. Fig. 9 shows time-lapse DIC images of contact formation (Fig. 9, columns *A–C*). Double labeling with FITC-phalloidin and E-cadherin antibody shows thin actin bundles directed towards individual puncta in these newly formed contact sites (*boxed areas*, Fig. 9, row *4*). Directly outside of the contact area, actin bundles are oriented towards the contact but are not associated with puncta (*open arrows*, Fig. 9, row *5*). Over 200 puncta were examined at newly established contact areas, and all were adjacent to actin (for example: *closed arrows*, Fig. 9, row *5*). These data suggest that there is an intimate association of actin filaments with E-cadherin/catenin puncta at initial stages of cell–cell adhesion.

FITC-phalloidin staining revealed cortical actin belts (diam. ~2 μm) that circumscribe single cells and boundaries of small colonies of cells (*open arrows*, Fig. 9 row *4*). Cortical actin belts between two contacting cells are present only in very young contacts (*open arrows*, Fig. 9, row *4*). At edges of mature contacts, actin bundles are directed towards bright clusters of TX-insoluble E-cadherin, with areas 10–100× larger than that of a single punctum at the boundary of the contact area (*closed white arrows*, Fig. 9, *C4* and *A4*). Careful observation of the DIC time-lapse movie of the right contact developing in Fig. 9, column *C* reveals breakage and reorganization of a structure with a thickness similar in dimensions to FITC-phalloidin stained actin belts (*arrows*, Fig. 9, rows *1–3*). Taken together, these data suggest that E-cadherin mediated adhesion results in rapid and dynamic reorganization of the cortical actin cytoskeleton.

Discussion

Contact formation between epithelial cells in vitro is an unpredictable and complex event. Many cells must be observed in order to capture the formation of one contact, and many individual contacts must be analyzed to obtain a sufficiently large data set to offset subtle variations in how contacts are formed. Computer-assisted, multi-site time-lapse DIC microscopy provides an experimental approach which enables analysis of formation of initial contacts between hundreds of cells at sufficient temporal and spatial resolution to observe membrane dynamics during cell–cell contact. Subsequently, retrospective confocal immunofluorescence microscopy can reveal protein distributions at high spatial resolution in the same contacts observed by time-lapse DIC microscopy. This type of analysis is an important partner to biochemical and structural analyses of protein–protein interactions (Hinck et al., 1994; Nagafuchi et al., 1994; Ozawa et al., 1990*b*; Shapiro et al., 1995; Wheelock et al., 1987), and quantitative assays of E-cadherin–mediated adhesion between cells (Angres et al., 1996). Together, these approaches have the potential to provide a detailed, mechanistic understanding of how specific proteins regulate cell–cell adhesion.

We describe in this report the dynamics of major proteins (E-cadherin, α-catenin, β-catenin, plakoglobin, and actin) known to be involved in Ca^{2+}-dependent adhesion during formation of epithelial cell–cell contacts. This analysis provides the first detailed picture of how the cadherin-catenin complex is recruited in time and space to cell–cell contacts, and the identification of macroscopic structures containing E-cadherin, α-catenin, β-catenin, and actin that may regulate specific steps in the initiation and strengthening of cell–cell adhesion. We have focused on the pool of E-cadherin, catenins and actin that is resistant to extraction with TX-100 since this pool of proteins has been shown to be critical for cell–cell adhesion. Previous studies have shown that cadherins and catenins are completely extracted from cells by Triton X-100 before formation of cell–cell contacts, and that cell–cell adhesion correlates with increased TX-100 insolubility and association of the cytoskeleton with these proteins (Nagafuchi and Takeichi, 1989; Ozawa et al., 1989; Shore and Nelson, 1991). Furthermore, deletion of the catenin binding site on cadherin, and hence linkage of cadherin to the cytoskeleton, prevents cell–cell adhesion and results in complete solubilization of cadherin by TX-100 (Nagafuchi and Takeichi, 1988; Ozawa et al., 1990*a*). Although we cannot rule out the possibility that some of the TX-100 insolubility of the E-cadherin/catenin complex is due to protein aggregation or incomplete lipid extraction, these previous results and those discussed below indicate a strong correlation between TX-100 insolubility and interaction with the actin cytoskeleton.

The TX-insoluble pools of E-cadherin, α-catenin, and β-catenin, but not plakoglobin (see below), accumulate rapidly and proportionally at initial cell–cell contact sites. This observation indicates that β-catenin, which binds both E-cadherin and α-catenin (Aberle et al., 1994; Jou et al.,

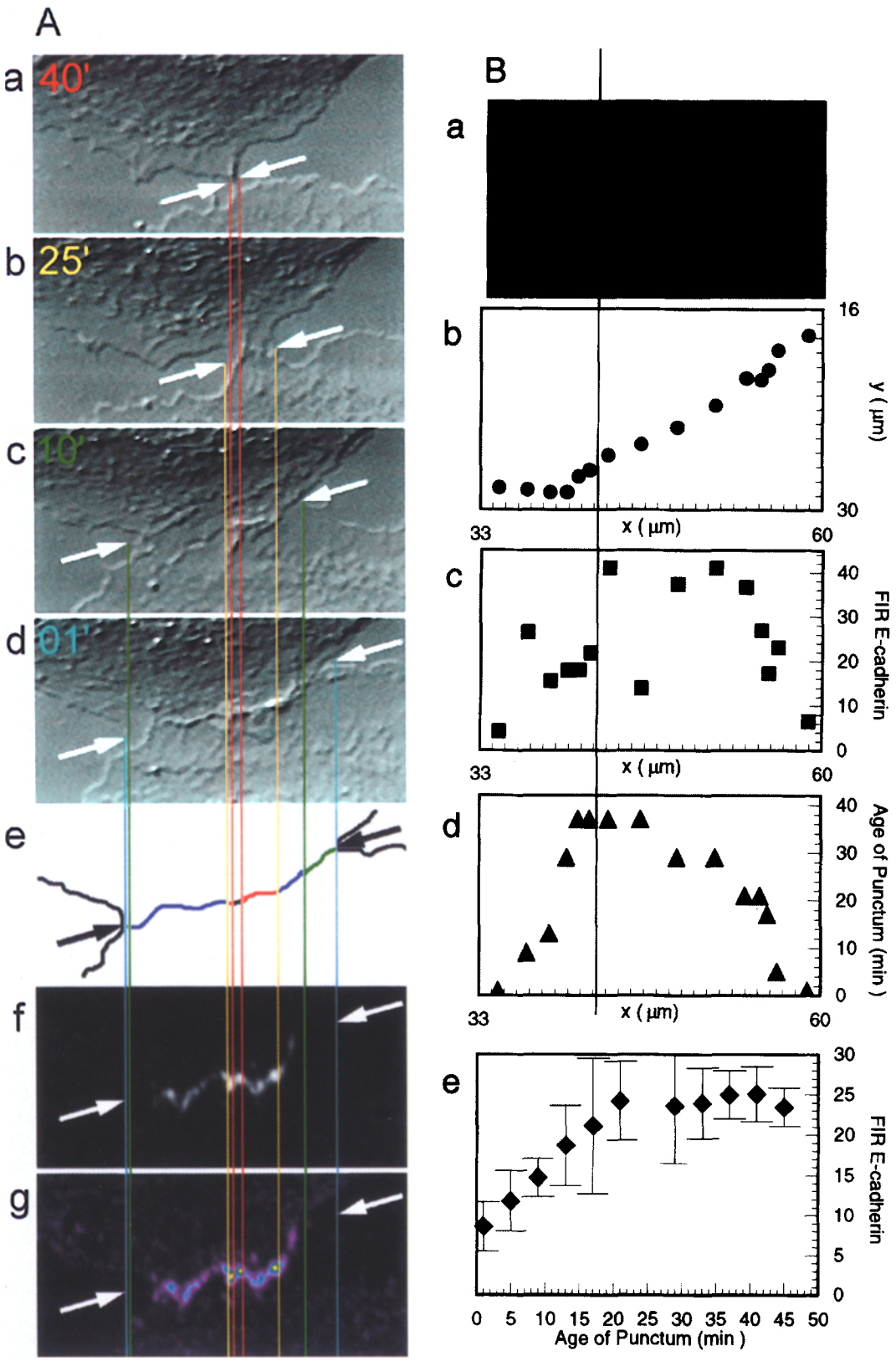

Figure 8. Accumulation of E-cadherin into puncta. (*A*) Determination of age along the length of a contact. DIC images (*a–d*) and a schematic representation (*e*) of a developing cell contact are shown. The age of a contact (min) is indicated in the upper left hand corner of each frame (*a*, 40 min; *b*; 25 min; *c*, 10 min; *d*, 1 min). The vertical lines running down the figure indicate the boundaries of the developing contact at each time point (between: red-red, >40′; red-yellow, 25′–40′; yellow-green, 10′–25′; green-blue, 0′–10′). The newly formed length of contact between frames is represented as the horizontal line between the arrows in *e* (black, >40′; red, 25′–40′; blue, 10′–25′; green, 0′–10′). For example, the additional contact length inserted between 40 and 25 min is represented by the area between

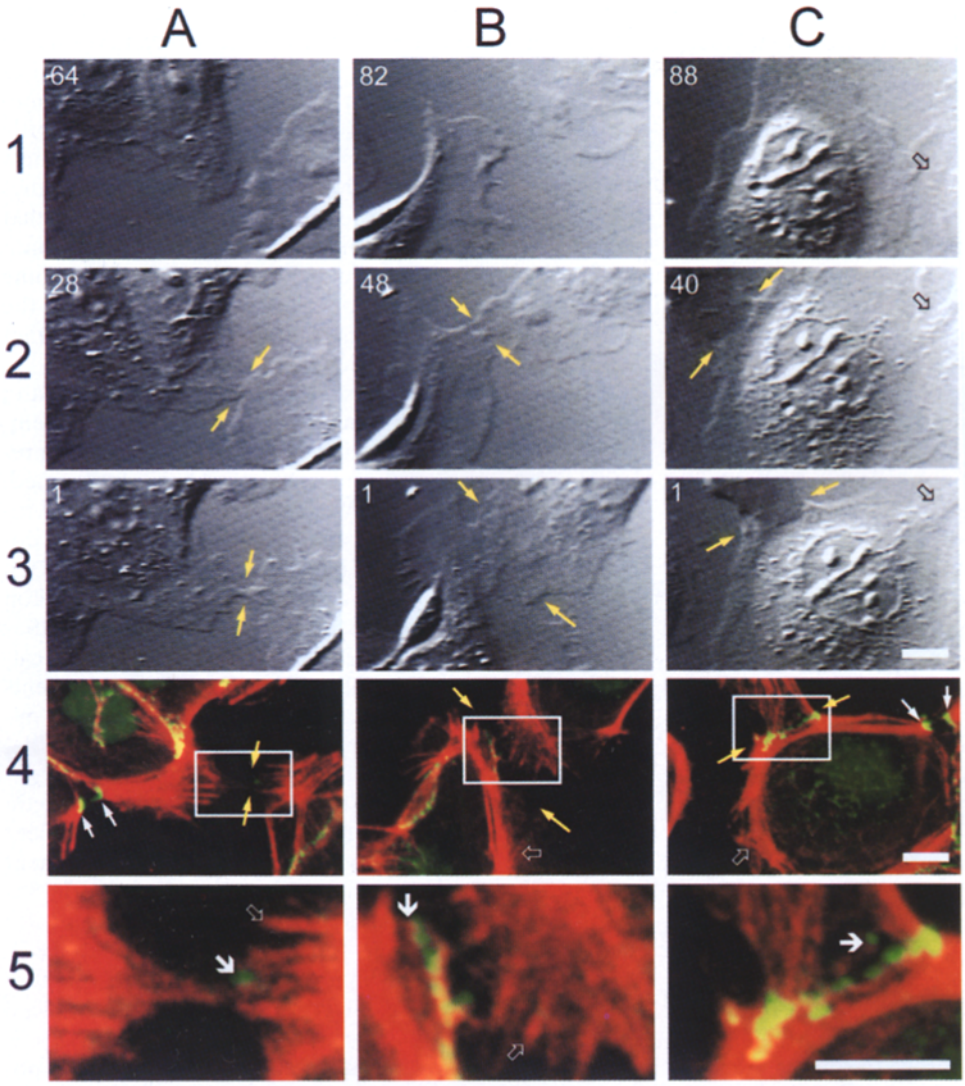

Figure 9. E-cadherin and actin distributions at cell–cell contacts. Cells were time-lapse imaged for 120 min, processed according to Materials and Methods, and labeled with E-cadherin and FITC-phalloidin. Rows *1–3* show time-lapse DIC images of contact formation; the time before fixation (min) is indicated at the top left hand corner of each panel and the developing contact is indicated between yellow arrows. The progression of the cortical actin belt to the periphery of the contact is indicated in column *C* by open arrows. Row *3* shows the last live DIC image. Row *4* shows retrospective fluorescence of E-cadherin (*green*) and actin (*red*). Yellow arrows point to the contact area; open white arrows in *B4* and *C4* point to actin belts during the initial stages of contact formation; closed white arrows in *A4* and *C4* point to actin belts which have reorganized to the edges of the contact and are associated with E-cadherin. Row *5* shows an enlargement of the boxed area in row *4*. Open arrows in row *5* point to actin bundles that are outside of the contact area and are not associated with puncta; closed arrows point to puncta near actin. Bar, 10 μm.

1995), and α-catenin, which binds actin (Rimm et al., 1995), coordinately assemble E-cadherin into the actin cytoskeleton during initial contact formation. Because different primary and secondary antibodies with different affinities were used in this study, we are unable to make quantitative measurements of protein stoichiometries in the complex. However, other reports have shown that E-cadherin, α-catenin, and β-catenin form a complex in a 1:1:1 protein ratio (Aberle et al., 1994; Hinck et al., 1994; Ozawa and Kemler, 1992). At present, we cannot determine whether E-cadherin, α-catenin, and β-catenin were present in a preformed, TX-100 soluble complex before cell–cell adhesion. However, pulse-chase studies of newly synthesized proteins in MDCK cells have shown that E-cadherin and β-catenin form a complex without α-catenin immediately following synthesis, and that α-catenin joins the complex at a time concordant with arrival of E-cadherin/β-catenin at the plasma membrane (Hinck et al., 1994). Furthermore, a complex of E-cadherin, α-catenin, and β-catenin can be isolated from cells in the absence of cell–cell contacts (Shore and Nelson, 1991). Together, these data indicate that the complex of E-cadherin, α-catenin, and β-catenin is preformed before initiation of cell–cell adhesion, and that the complex is recruited into a TX-insoluble pool following initiation of cell adhesion.

Plakoglobin binds to both E-cadherin and α-catenin (Aberle et al., 1994; Hinck et al., 1994), and to members of the cadherin super-family in desmosomes (Magee and Buxton, 1991; Troyanovsky et al., 1994). However, the role of plakoglobin in E-cadherin–mediated cell adhesion

the vertical red and yellow lines throughout the image, and the red horizontal lines between the arrows in *e*. Puncta which are in this region are considered to be 25–40-min-old: retrospective E-cadherin staining of the contact is shown in *f*, and in pseudocolor format in *g*. (*B*) Kinetics of E-cadherin accumulation into puncta. FIR of all puncta in an individual contact, and the age of each segment of that contact were calculated. (*a*) E-Cadherin immunofluorescence of a 45-min-old contact. (*b*) (x, y) coordinate representation of the puncta in the contact. Note that some puncta are not boxed and were not analyzed because they were too close to other puncta. FIR (*c*) and age (*d*) of each punctum is graphed as a function of the position of each punctum along the contact. Graph *e* shows FIR values from five contacts averaged as a function of the age of each punctum; error bars represent the standard error of the mean.

is poorly understood. Our study shows that during initial formation of MDCK cell–cell contacts plakoglobin neither accumulates in a TX-insoluble pool, nor colocalizes with E-cadherin, α-catenin, and β-catenin. Interestingly, pulse-chase studies have revealed that E-cadherin/β-catenin and E-cadherin/plakoglobin complexes are formed equally following synthesis in MDCK cells (Hinck et al., 1994). If both complexes exist at the plasma membrane before cell–cell contact, our results indicate that the E-cadherin/β-catenin complex is preferentially, if not exclusively, involved in initiation of cell adhesion between MDCK cells. We note, however, that plakoglobin is associated with cell–cell contacts at later times in a TX-insoluble pool, which may reflect the interaction of plakoglobin with desmosome cadherin complexes that form after initial E-cadherin–mediated cell–cell contact (Jones and Green, 1991; Magee and Buxton, 1991; Pasdar and Nelson, 1988). Taken together, these data imply that β-catenin plays a role in formation of new contacts, while plakoglobin is involved in the subsequent stabilization of contacts (see also Lampugnani et al., 1995). Extending the time-lapse imaging period to examine maturation of contacts (12–24 h) may resolve the time at which plakoglobin, and the many other junctional complex proteins enter the cell–cell contact area.

The time course of recruitment of E-cadherin, α-catenin, and β-catenin into a TX-100 complex following initiation of cell–cell adhesion is rapid; the relative amounts of each protein at individual contacts and puncta reached a maximum after ~30–40 min, with a half-time ($t_{1/2}$) of ~15–20 min (Figs. 3 and 8 *B*). This time course is remarkably similar to that for strengthening of adhesion reported recently by Angres et al. (1996) using a very different experimental approach. By measuring the development of adhesive strength between fibroblasts expressing E-cadherin, Angres et al. (1996) showed that maximum adhesion strength between cells was attained ~40 min after initial contact with a $t_{1/2}$ of ~15 min. That TX-insoluble E-cadherin, α-catenin, and β-catenin accumulate proportionally and coordinately at newly established contact sites and individual puncta (this study) in a time course identical to that for strengthening of adhesion suggests that binding of the E-cadherin/catenin complex to the actin cytoskeleton determines the kinetics of strengthening of adhesion during initial cell–cell contact formation.

How does formation of TX-insoluble complexes containing E-cadherin, α-catenin, and β-catenin at cell–cell contacts result in initiation and strengthening of cell adhesion? In this study, we show that TX-insoluble E-cadherin, α-catenin, and β-catenin colocalize and coaccumulate in discrete macroscopic puncta along contacts between cells. These puncta are not an artifact of membrane extraction with TX-100 since distinct morphological structures of similar distributions and dimensions were observed at contacts between living cells by DIC microscopy (Fig. 5), and following different conditions of fixation and detergent extraction (data not shown). We believe that initial stabilization of the contact results from the successful nucleation of a punctum and that new puncta are added to the contact area as it grows. In addition we know that in these early contacts the density of puncta (i.e., the number of puncta per unit length) is approximately constant (Fig. 6 *a*), and that the density of new puncta added to the developing contact is proportional to the new length. Significantly, puncta coaccumulate E-cadherin, α-catenin, and β-catenin as they are formed along the developing contact, and as one protein accumulates in a punctum, the others accumulate stoichiometrically (Figs. 7 and 8). We know very little about the lifetime of a punctum, how it is nucleated, how it's size is constrained, or how long it exists; these studies are beyond the scope of the present study. We suggest that accumulation of E-cadherin, α-catenin, and β-catenin into sites of contact formation depends on the amount of time puncta have been in the contact, while the strength of the contact increases by spacing multiple puncta at constant average density along the length of the contact.

Although the actin cytoskeleton has been implicated in the formation of cadherin mediated cell adhesion, the temporal and spatial organization of cadherins and actin in relation to initial cell–cell contacts has not been determined. Cells expressing an E-cadherin mutant that contains cytoplasmic domain deletions but an intact extracellular domain (Nagafuchi and Takeichi, 1988; Ozawa et al., 1990*a*), or intact E-cadherin but a disrupted actin cytoskeleton (Angres et al., 1996), are poorly adherent. Our studies show that puncta containing TX-insoluble E-cadherin, α-catenin, and β-catenin are localized very close to actin filaments in the contact site (Fig. 9). Early studies with electron microscopy showed a similar localization of actin microfilaments with initial cell–cell contacts in fibroblasts (Heaysman and Pegrum, 1973). These data imply a role for actin in coordinating the formation and constant average density of these adhesive structures during the development of cell–cell adhesion. In mature contacts, E-cadherin has been observed in association with a cortical ring of actin filaments at the adherens junction (Hirano et al., 1987), and at the ends of actin bundles in fibroblasts (Yonemura et al., 1995). Individual puncta resolved in early cell–cell contacts may eventually coalesce to form the adherens junction that circumscribes the apical junction in fully polarized epithelial cells. Whether or not attachment of actin bundles to puncta in the adherens junction is at the ends of filaments or laterally along the side of filaments remains unknown. However, we hypothesize that actin is involved in both stabilizing and limiting the size of puncta: the cadherin/catenin complex may use actin as an anchor and be constrained by the dimensions of the actin bundle. This type of mechanical linkage at cell–cell contacts would allow the cell to rapidly restructure small areas of contacting membrane while maintaining strong adhesion throughout the remaining contacting edges.

Concentrating E-cadherin/catenin complexes into puncta may be important for strengthening adhesion during initial cell–cell contact by locally increasing the inherent low affinity of E-cadherin extracellular domains on opposing membranes. Studies of complexes of recombinant extracellular E-cadherin have shown that the affinity of homotypic E-cadherin binding is weak (Shapiro et al., 1995). Clustering and immobilizing large numbers of E-cadherin/catenin complexes may result in increased numbers of rebinding events per area, or conformational changes in E-cadherin which increase homotypic binding affinity. Since clustering of E-cadherin and strengthening of adhesion are dependent on actin in vivo, the association of E-cadherin/catenin complexes with actin filaments may be required for

stabilizing crystalline arrays of E-cadherin within these puncta, and, thereby, strengthening the adhesive contact between cells.

We are grateful to Chris Hazuka and members of the Smith and Nelson labs for their comments during the course of this work.

This work was supported by funds from the National Institutes of Health (NIH) (NS28587) and NIMH Silvio Conte Center for Neuroscience Research (MH48104) to S. J. Smith, the NIH (GM35527) to W.J. Nelson, and Mathers Charitable Foundation to S.J. Smith and W.J. Nelson.

Received for publication 29 July 1996 and in revised form 2 October 1996.

References

Aerle, H., S. Butz, J. Stappert, H. Weissig, R. Kemler, and H. Hoschuetzky. 1994. Assembly of the cadherin-catenin complex in vitro with recombinant proteins. *J. Cell Sci.* 107:3655–3663.

Angres, B., A. Barth, and W.J. Nelson. 1996. Mechanism for transition from initial to stable cell–cell adhesion: kinetic analysis of E-cadherin–mediated adhesion using a quantitative adhesion assay. *J. Cell Biol.* 134:549–557.

Behrens, J., W. Birchmeier, S. Goodman, and B. Imhof. 1985. Dissociation of Madin-Darby canine kidney epithelial cells by the monoclonal antibody anti–arc-1: mechanistic aspects and identification of the antigen as a component related to uvomorulin. *J. Cell Biol.* 101:1307–1315.

Breen, E., G. Steele, and A. Mercurio. 1994. A functional cadherin-catenin complex is associated with a decrease in colon carcinoma cell proliferation. *Surg. Forum.* 45:507–509.

Butz, S., J. Stappert, H. Weissig, R. Kemler, P.D. McCrea, C.W. Turck, and B. Gumbiner. 1992. Plakoglobin and β-catenin are distinct but closely related. *Science (Wash. DC).* 257:1142–1144.

Friedlander, D., R. Mege, B. Cunningham, and G. Edelman. 1989. Cell sorting-out is modulated by both the specificity and amount of different cell adhesion molecules (CAMs) expressed on cell surfaces. *Proc. Natl. Acad. Sci. USA.* 86:7043–7047.

Gumbiner, B., B. Stevenson, and A. Grimaldi. 1988. The role of the cell adhesion molecule uvomorulin in the formation and maintenance of the epithelial junctional complex. *J. Cell Biol.* 107:1575–1587.

Herrenknecht, K., M. Ozawa, C. Eckerskorn, F. Lottspeich, M. Lenter, and R. Kemler. 1991. The uvomorulin-anchorage protein α-catenin is a vinculin homologue. *Proc. Natl. Acad. Sci. USA.* 88:9156–9160.

Heaysman, J. E., and S. M. Pegrum. 1973. Early contacts between fibroblasts. *Exp. Cell Res.* 78:71–78.

Hinck, L., I. Nathke, J. Papkoff, and W.J. Nelson. 1994. Dynamics of cadherin/catenin complex formation: novel protein interactions and pathways of complex assembly. *J. Cell Biol.* 125:1327–1340.

Hirano, S., N. Kimoto, Y. Shmoyama, S. Hirohashi, and M. Takeichi. 1992. Identification of a neural α-catenin as a key regulator of cadherin function and multicellular organization. *Cell.* 70:293–301.

Hirano, S., A. Nose, K. Hatta, A. Kawakami, and M. Takeichi. 1987. Calcium-dependent cell–cell adhesion molecules (cadherins): subclass specificities and possible involvement of actin bundles. *J. Cell Biol.* 105:2501–2510.

Jaffe, S., D. Friedlander, F. Matsuzaki, K. Crossin, B. Cunningham, and G. Edelman. 1990. Differential effects of the cytoplasmic domains of cell adhesion molecules on cell aggregation and sorting-out. *Proc. Natl. Acad. Sci. USA.* 87:3589–3593.

Jones, J.C., and K.J. Green. 1991. Intermediate filament-plasma membrane interactions. *Curr. Opin. Cell Biol.* 3:127–132.

Jou, T.-S., D. Stewart, J. Stappert, W.J. Nelson, and J. Marrs. 1995. Genetic and biochemical dissection of protein linkages in the cadherin-catenin complex. *Proc. Natl. Acad. Sci. USA.* 92:5067–5071.

Lampugnani, M., M. Corada, L. Caveda, F. Breviario, O. Ayalon, B. Feigher, and E. Dejana. 1995. The molecular organization of endothelial cell–cell junctions: differential association of plakoglobin, β-catenin, and α-catenin with vascular endothelial cadherin (VE-cadherin). *J. Cell Biol.* 129:203–217.

Magee, A., and R. Buxton. 1991. Transmembrane molecular assemblies regulated by the greater cadherin family. *Curr. Opin. Cell Biol.* 3:854–861.

Matsuzaki, F., R. Mege, S. Jaffe, D. Freidlander, W. Gallin, J. Goldberg, B. Cunningham, and G. Edelman. 1990. cDNAs of cell adhesion molecules of different specificity induce changes in cell shape and border formation in cultured s180 cells. *J. Cell Biol.* 110:1239–1252.

Mays, R.W., K.A. Siemers, B.A. Fritz, A.W. Lowe, C. van Meer, and W.J. Nelson. 1995. Hierarchy of mechanisms involved in generating Na/K-ATPase polarity in MDCK epithelial cells. *J.Cell Biol.* 130:1105–1115.

McCrea, P., C. Turck, and B. Gumbiner. 1991. A homologue of the *armadillo* protein in *Drosophila* (plakoglobin) associated with E-cadherin. *Science (Wash. DC).* 254:1359–1361.

McNeill, H., M. Ozawa, R. Kemler, and W.J. Nelson. 1990. Novel function of the cell adhesion molecule uvomorulin as an inducer of cell surface polarity. *Cell.* 62:309–316.

McNeill, H., T. Ryan, S. J. Smith, and W.J. Nelson. 1993. Spatial and temporal dissection of immediate and early events following cadherin-mediated epithelial cell adhesion. *J. Cell Biol.* 120:1217–1226.

Mege, R., F. Matsuzaki, W. Gallin, J. Goldberg, B. Cunningham, and G. Edelman. 1988. Construction of epithelioid sheets by transfection of mouse sarcoma cells with cDNAs for chicken cell adhesion molecules. *Proc. Natl. Acad. Sci. USA.* 85:7274–7278.

Nagafuchi, A., and M. Takeichi. 1988. Cell binding function of E-cadherin is regulated by the cytoplasmic domain. *EMBO (Eur. Mol. Biol. Organ.) J.* 7: 3679–3684.

Nagafuchi, A., and M. Takeichi. 1989. Transmembrane control of cadherin-mediated cell adhesion: a 94Kd protein functionally associated with a specific region of the cytoplasmic domain of E-cadherin. *Cell Regulation.* 1:37–44.

Nagafuchi, A., Y. Shirayoshi, K. Okazaki, K. Yasuda, and M. Takeichi. 1987. Transformation of cell adhesion properties by exogenously introduced E-cadherin cDNA. *Nature (Lond.).* 329:341–343.

Nagafuchi, A., M. Takeichi, and S. Tsukia. 1991. The 102 Kd cadherin-associated protein: similarity to vinculin and posttranscriptional regulation of expression. *Cell.* 65:849–857.

Nagafuchi, A., S. Ishihara, and S. Tsukita. 1994. The roles of catenins in the cadherin-mediated cell adhesion: functional analysis of E-cadherin-α-catenin fusion molecules. *J. Cell Biol.* 127:235–245.

Nathke, I.S., L. Hinck, J.R. Swedlow, J. Papkoff, and W.J. Nelson. 1994. Defining interactions and distributions of cadherin and catenin complexes in polarized epithelial cells. *J. Cell Biol.* 125:1341–1352.

Nelson, W.J., and P.J. Veshnock. 1986. Dynamics of membrane-skeleton (fodrin) organization during development of polarity in Madin-Darby canine kidney epithelial cells. *J. Cell Biol.* 103:1751–1765.

Nose, A., A. Nagafuchi, and M. Takeichi. 1988. Expressed recombinant cadherins mediate cell sorting in model systems. *Cell.* 54:993–1001.

Nose, A., K. Tsuji, and M. Takeichi. 1990. Localization of specificity determining sites in cadherin cell adhesion molecules. *Cell.* 61:147–155.

Oyama, T., Y. Kanai, A. Ochiai, S. Akimoto, T. Oda, K. Yanagihara, A. Nagafuchi, S. Tsukia, S. Shibamoto, F. Ito, et al. 1994. A truncated β-catenin disrupts the interaction between E-cadherin and α-catenin: a cause of loss of intercellular adhesiveness in human cancer cell lines. *Cancer Res.* 54:6282–6287.

Ozawa, M., and R. Kemler. 1992. Molecular organization of the uvomorulin-catenin complex. *J. Cell Biol.* 116:989–996.

Ozawa M., H. Baribault, and R. Kemler. 1989. The cytoplasmic domain of the cell adhesion molecule uvomorulin associates with three independent proteins structurally related in different species. *EMBO (Eur. Mol. Biol. Organ.) J.* 8:1711–1717.

Ozawa, M., J. Engel, and R. Kemler. 1990*a*. Single amino acid substitutions in one Ca^{2+} binding site of uvomorulin abolish the adhesive function. *Cell.* 63:1033–1038.

Ozawa, M., M. Ringwald, and R. Kemler. 1990*b*. Uvomorulin-catenin complex formation is regulated by a specific domain in the cytoplasmic region of the cell adhesion molecule. *Proc. Natl. Acad. Sci. USA.* 87:4246–4250.

Pasdar, M., and W.J. Nelson. 1988. Kinetics of desmosome assembly in Madin-Darby canine kidney epithelial cells: temporal and spatial regulation of desmoplakin organization and stabilization upon cell–cell contact. I. Biochemical analysis. *J. Cell Biol.* 106:677–685.

Rimm, D., E. Koslov, P. Kebriaei, C. Cianci, and J. Morrow. 1995. α_1(E)-Catenin is an actin-binding and -bundling protein mediating the attachment of F-actin to the membrane adhesion complex. *Proc. Natl. Acad. Sci. USA.* 92:8813–8817.

Salas, P.J., D. Vega-Salas, J. Hochman, E. Rodriguez-Boulan, and M. Edidin. 1988. Selective anchoring in the specific plasma membrane domain: a role in epithelial cell polarity. *J. Cell Biol.* 107:2363–2376.

Shapiro, L., A.M. Fannon, P.D. Kwong, A. Thompson, M.S. Lehmann, G. Grubel, J. Legrand, J. Als-Nielsen, D.R. Colman, and W.A. Hendrickson. 1995. Structural basis of cell–cell adhesion by cadherins. *Nature (Lond.).* 372:327–374.

Shimoyama, Y., A. Nagafuchi, S. Fujita, M. Gotoh, M. Takeichi, S. Tsukia, and S. Hirohashi. 1992. Cadherin dysfunction in a human cancer cell line: possible involvement of loss of α-catenin expression in reduced cell–cell adhesiveness. *Cancer Res.* 52:5770–5774.

Shore, E., and W.J. Nelson. 1991. Biosynthesis of the cell adhesion molecule uvomorulin (E-cadherin) in Madin-Darby canine kidney epithelial cells. *J. Biol. Chem.* 266:19672–19680.

Stappert, J., and R. Kemler. 1994. A short region of E-cadherin is essential for catenin binding and is highly phosphorylated. *Cell Adh. Comm.* 2:319–327.

Takeichi, M. 1991. Cadherin cell adhesion receptors as a morphogenetic regulator. *Science (Wash. DC).* 251:1451–1455.

Takeichi, M., K. Hatta, A. Nose, and A. Nagafuchi. 1988. Identification of a gene family of cadherin cell adhesion molecules. *Cell Differ. Dev.* 25:91–94.

Troyanovsky, S., R. Troyanovsky, L. Eshkind, V. Krutovskikh, R. Leube, and W.W. Franke. 1994. Identification of the plakoglobin-binding domain on desmoglein and its role in plaque assembly and intermediate filament anchorage. *J. Cell Biol.* 127:151–160.

Tsukita, S., S. Tsukita, A. Nagafuchi, and S. Yonemura. 1992. Molecular linkage between cadherins and actin filaments in cell–cell adherens junctions. *Curr. Opin. Cell Biol.* 4:834–839.

Wheelock, M.J., C.A. Buck, K.B. Bechtol, and C.H. Damsky. 1987. Soluble 80-Kd fragment of Cell-CAM 120/80 disrupts cell–cell adhesion. *J. Cell. Biochem.* 34:187–202.

Yonemura, S., M. Itoh, A. Nagafuchi, and S. Tsukita. 1995. Cell-to-cell adherens junction formation and actin filament organization: similarities and differences between non-polarized fibroblasts and polarized epithelial cells. *J. Cell Sci.* 108:127–142.